Appl. Phys. B 81, 1107–1111 (2005)
DOI: 10.1007/s00340-005-1959-2

Applied Physics B
Lasers and Optics

Y. DENG[1,✉]
C. WANG[1]
L. CHAI[1]
Z. ZHANG[1,2]

Determination of Gabor wavelet shaping factor for accurate phase retrieval with wavelet-transform

[1] Ultrafast Laser Laboratory, School of Precision Instrument and Optoelectronics Engineering, Key Laboratory of Optoelectronics Information Technical Science, EMC, Tianjin University, Tianjin 300072, P.R. China
[2] Institute of Quantum Electronics, School of Electronics Engineering and Computer Science, Peking University, Beijing 100871, P.R. China

Received: 15 May 2005/Revised version: 12 July 2005
Published online: 22 October 2005 •

ABSTRACT We examined the range of shape factor of the Gabor wavelet in the analysis of spectral phase retrieval with an interferogram. We demonstrated that for the pulses with moderate high order phase the accuracy of the retrieved phase is insensitive to the shaping factor in the range of $1 \sim 20$. Both simulated ideal Gaussian spectrum and actual non-Gaussian spectrum are applied in the analysis.

PACS 42.65.Re; 42.30.Rx

1 Introduction

Time-frequency analysis is an effective tool for characterizing the time-varying spectral components of signals. Recently, we introduced wavelet-transform (WT) [1, 2] into the spectral phase retrieval of femtosecond pulses [3, 4]. The signal is collected with spectral phase interferometry for direct electric-field reconstruction (SPIDER) apparatus [5], and part of the phase retrieval procedure is also similar to SPIDER process. In the conventional SPIDER phase retrieval procedure [5], there are three peaks after Fourier transform (FT) of the spectral interferogram (SI). A super-Gaussian type filter is applied centered one of the AC terms. Select a reasonable filter widths, the phase is retrieved after a seconded FT [6]. However a different filter introduces different noises, which creates uncertainty in phase retrieval. Wavelet-transform analysis for spectral phase extraction does not need a filter in time domain; therefore, the uncertainty introduced by the temporal filter is avoided. On the other hand, the time-frequency analysis is similar to frequency resolved optical gating (FROG) technique [7]. In the spectrogram of FROG trace, the time domain phase (chirp) can be directly identified; and WT of SI also results two two-dimensional time-frequency topographies (an amplitude topography and a phase topography) [3], the frequency domain phase (spectral phase) can be also directly identified from the amplitude topography. However, the phase retrieval algorithm of FROG needs the procedure of iterative, but the phase extraction procedure of WT algorithm is non-iterative.

✉ Fax: +86-22-27404204, E-mail: yuqdeng@yahoo.com

Different from FT [6], the basis of WT is not unique. To extract spectral phase from SI, a complex mother wavelet is needed to the analysis. The most widely used complex wavelet is the Gabor wavelet whose shape is controlled by a single parameter named as the shaping factor [8]. One can imagine that the shaping factor of the Gabor wavelet, which controls the time-frequency localization property, should strongly influence the effectiveness of WT analysis. Therefore, it is important to examine how the shaping factor affects the retrieved phase, for the best restoring the phase from SI.

2 Brief introduction of Gabor wavelet

In any case of signal analysis, one must take in consideration two resolutions: the time resolution and the frequency resolution. However, one cannot improve both simultaneously: when the time resolution is improved, the frequency resolution must be degraded; likewise, when the frequency resolution is improved, the time resolution must be degraded. This is like the Heisenberg's Uncertainty Principle. The signal analysis accuracy is confined in a box, the vertical dimension of the box denotes the accuracy of time, $\Delta\tau$, and the horizontal dimension denotes the accuracy of frequency, $\Delta\nu$; whereas the area of the box is prescribed, i.e., $\Delta\tau\Delta\nu$ is a constant. We called this box the Heisenberg Box.

The Gabor wavelet is one of the most widely used analytic wavelets. It has the best time-frequency resolution, i.e., the smallest Heisenberg box. It is a complex frequency-modulated Gaussian function, which can be expressed as [8]:

$$\psi(t) = \frac{1}{(\sigma^2\pi)^{1/4}} \mathrm{e}^{-\frac{t^2}{2\sigma^2}+\mathrm{i}\eta t} \tag{1}$$

There are two parameters in (1): time spread σ and center frequency η. However, the shape of the mother Gabor wavelet can be characterized by a single dimensionless parameter called the Gabor wavelet shaping factor, Gs, which is defined as $Gs = \sigma\eta$ [8].

By adjusting the values of Gs, the desired shape of Gabor wavelet can be obtained. Morlet wavelet, another commonly used wavelet, is a special case of Gabor wavelet. The shaping factor for the most widely used Morlet wavelet is $Gs = 5$ ($\sigma = 1$ and $\eta = 5$).

Gabor wavelet shaping factor not only determines the shape of wavelet, but also controls the time-frequency reso-

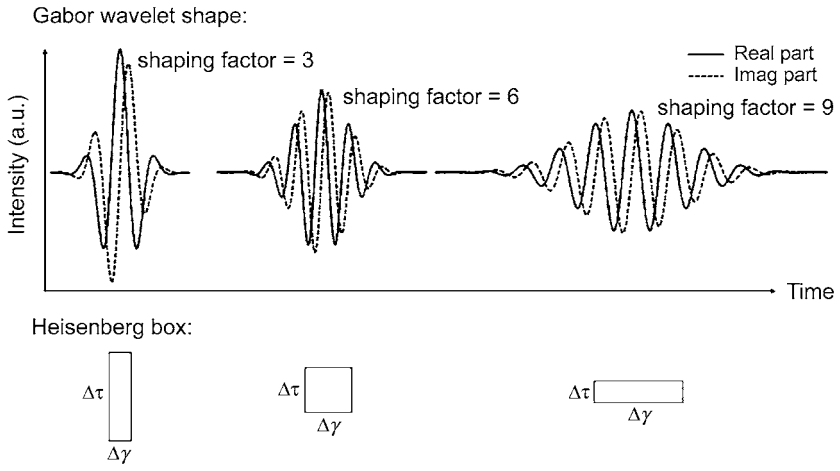

FIGURE 1 The Gabor wavelet profile has more oscillations as the shaping factor is from small to large. The "Heisenberg box" shows the relationship between the temporal resolution and the frequency resolution, like the principle of uncertainty in quantum mechanics

lution, via the shape of the Heisenberg box. The shape of the Gabor wavelet and the "Heisenberg box" with the shaping factors of 3, 6 and 9 are shown in Fig. 1, respectively. The larger shaping factor means more oscillations under the wavelet envelope, and a larger dimension in horizontal axis. Therefore the time resolution degrades, and the frequency resolution improved as the shaping factor increases. Like in the quantum mechanics, the smaller shaping factor wavelet has a high frequency resolution but loses the time resolution: one cannot have high resolutions for both simultaneously. The above fact gives us a hint: the shaping factor of the wavelet might have a tricky influence on the phase retrieval. Let us examine the phase retrieval with different shape of Gabor wavelet.

3 Brief review of wavelet-transform for phase extraction from spectral interferogram

Wavelet-transform is the inner scalar between signal and daughter wavelet functions [1, 2]. If a function, $\psi(t)$, is selected as mother wavelet, the daughter wavelets generation from dilations and translations of it can be expressed as:

$$\psi_{a,b}(t) = \psi\left(\frac{t-b}{a}\right), \tag{2}$$

where a is the dilation factor, and b the translation factor.

In a SPIDER apparatus, the interferogram is generated from spectral shearing interference, which can be expressed as [5]:

$$f(\omega) = \left|\tilde{E}(\omega_c - \Omega)\right|^2 + \left|\tilde{E}(\omega_c)\right|^2 + 2\left|\tilde{E}(\omega_c - \Omega)\right| \cdot \left|\tilde{E}(\omega_c)\right| \times \cos[\omega\tau + \theta(\omega_c)], \tag{3}$$

where $\theta(\omega_c) = \varphi_\omega(\omega_c - \Omega) - \varphi_\omega(\omega_c)$ is the spectral phase difference, $\Omega = -\tau/\ddot{\varphi}$ spectral shearing, τ pulses time delay between the two replicas, and $\ddot{\varphi}$ the two-order dispersion of the stretcher. $\tilde{E}(\omega_c - \Omega)$ and $\tilde{E}(\omega_c)$ are the spectra of the two replicas.

When WT is applied in the spectral phase extraction from SI $f(\omega')$, it takes the following form [3, 4]:

$$W(\Delta\omega, \omega) = \frac{1}{\Delta\omega}\int_{-\infty}^{+\infty} f(\omega')\psi^*\left(\frac{\omega' - \omega}{\Delta\omega}\right) \mathrm{d}\omega' \tag{4}$$

where $\psi^*[(\omega' - \omega)/\Delta\omega]/\Delta\omega$ is the complex conjugation of daughter wavelet $\psi[(\omega' - \omega)/\Delta\omega]/\Delta\omega$, $\Delta\omega$ is a dilation factor that represents a variable width of the daughter wavelet, for measuring the spacing of the interferogram, and ω the translation factor that shifts the peak of the daughter wavelet along the interferogram.

Based on (4), WT of a SI produces a two-dimensional complex array, which can be plotted as two two-dimensional topographies: an amplitude topography and a phase topography, in which $\Delta\omega$ corresponding to time ($t = 2\pi/\Delta\omega$) and ω corresponding to frequency. To retrieve the phase of femtosecond optical pulses, we first find the maximum value of the amplitude topography of WT along frequency direction [3]. This curve of maximum on the amplitude topography is like a ridgeline of a mountain; therefore we called it as the ridgeline of WT [9]. This ridgeline is then projected onto the phase topography, with which the folded spectral phase is extracted along projected ridgeline.

4 Influence of shaping factor on the spectral phase retrieval

In this section we assume a Gaussian type femtosecond pulse, with a Gaussian type spectrum. The transform limited pulse width is 13.90 fs and the spectrum has a bandwidth (FWHM) of 68.03 nm (31.83 THz), centered at 800 nm. Assume the following three phases are applied to the pulse, which are respectively shown in Fig. 2a.

Phase 1 $\varphi(\omega) = 200\,\mathrm{fs}^2 \times (\omega - \omega_0)^2$

Phase 2 $\varphi(\omega) = 200\,\mathrm{fs}^2 \times (\omega - \omega_0)^2 - 600\,\mathrm{fs}^3 \times (\omega - \omega_0)^3$

Phase 3 $\varphi(\omega) = 200\,\mathrm{fs}^2 \times (\omega - \omega_0)^2 - 600\,\mathrm{fs}^3 \times (\omega - \omega_0)^3 + 12\,000\,\mathrm{fs}^4 \times (\omega - \omega_0)^4$

The pulse will be stretched to 80.90 fs, 25.46 fs and 60.78 fs in time domain, which are respectively shown in Fig. 2b.

We can make the SI with the above assumed spectrum, spectral phases, and with different SPIDER parameters: the time delay of the pulse pair τ and the spectral shear Ω, which are:

Case 1: Time delay $\tau = 0.7$ ps

and spectral shearing $\Omega = 22.0 \times 10^{12}$ rad/s;

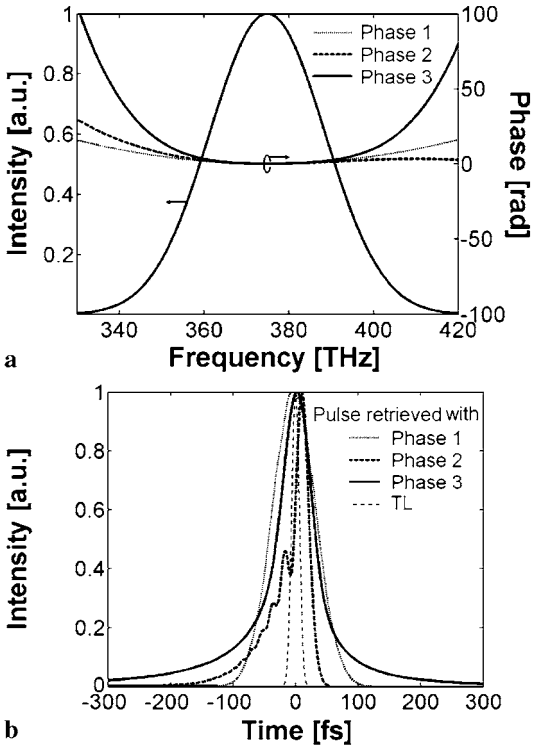

FIGURE 2 Simulated spectrum and assumed phases. **(b)** Pulse profiles reconstructed with simulated spectrum and assumed phases, TL: transform-limited pulse

Case 2: Time delay $\tau = 1.0\,\text{ps}$

and spectral shearing $\Omega = 31.4 \times 10^{12}\,\text{rad/s}$.

Then we calculate the spectral phase with WT ridge algorithm [3, 9]. The WT ridges of the SI for the given phases and the corresponding "Heisenberg boxes" are shown in Fig. 3.

To evaluate the accuracy for different shaping factors, we introduce the relative phase error ε_φ defined as:

$$\varepsilon_\varphi = \frac{\int_{-\infty}^{+\infty} |\varphi_r(\omega) - \varphi_0(\omega)| \cdot I(\omega)\,\mathrm{d}\omega}{\int_{-\infty}^{+\infty} |\varphi_0(\omega)|\, I(\omega)\,\mathrm{d}\omega}, \tag{5}$$

where $\varphi_r(\omega)$ the retrieved phase, $\varphi_0(\omega)$ the given phase, and $I(\omega)$ the intensity of the spectrum.

We vary the shaping factor from 1 to 20 of Gabor wavelet to retrieve the spectral phases. The retrieval errors for the three phases are shown in Fig. 4.

Figure 4 shows the retrieval errors with different Gabor wavelet shaping factors. For the phase 1, the spectral phase can be precisely retrieved with a relative phase errors less than 1%, in a large shaping factor range of $2 \sim 20$. For the phase 2, the retrieval phase error is also less than 1% in the shaping factor range of $2 \sim 15$, and the retrieval phase error slightly increases with the shaping factor. However, for the phase 3, the spectral phase can be retrieved only in a relatively narrow shaping factor range of $2 \sim 7$. For a shaping factor of more than 7, the retrieval phase error increases sharply.

To demonstrate that this method can be used in actual femtosecond laser pulses, we took a practical spectrum from

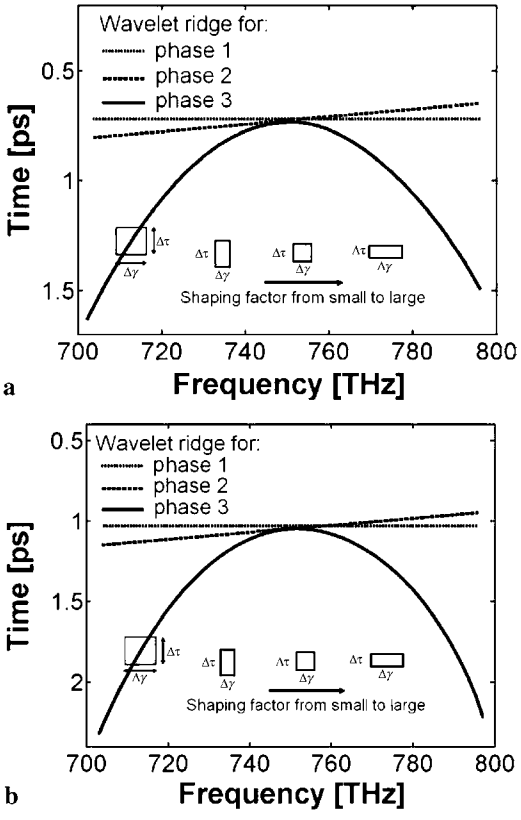

FIGURE 3 Wavelet-transform ridges of the spectral interferogram for the given phases. **(a)** Time delay $\tau = 0.7$ ps. **(b)** Time delay $\tau = 1.0$ ps

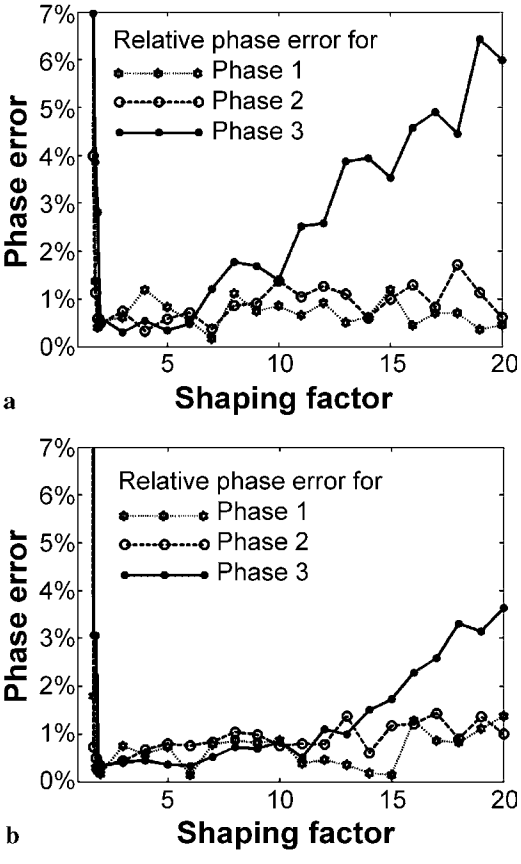

FIGURE 4 Phase errors retrieved by Gabor mother wavelet with different shaping factor. **(a)** Time delay $\tau = 0.7$ ps. **(b)** Time delay $\tau = 1.0$ ps

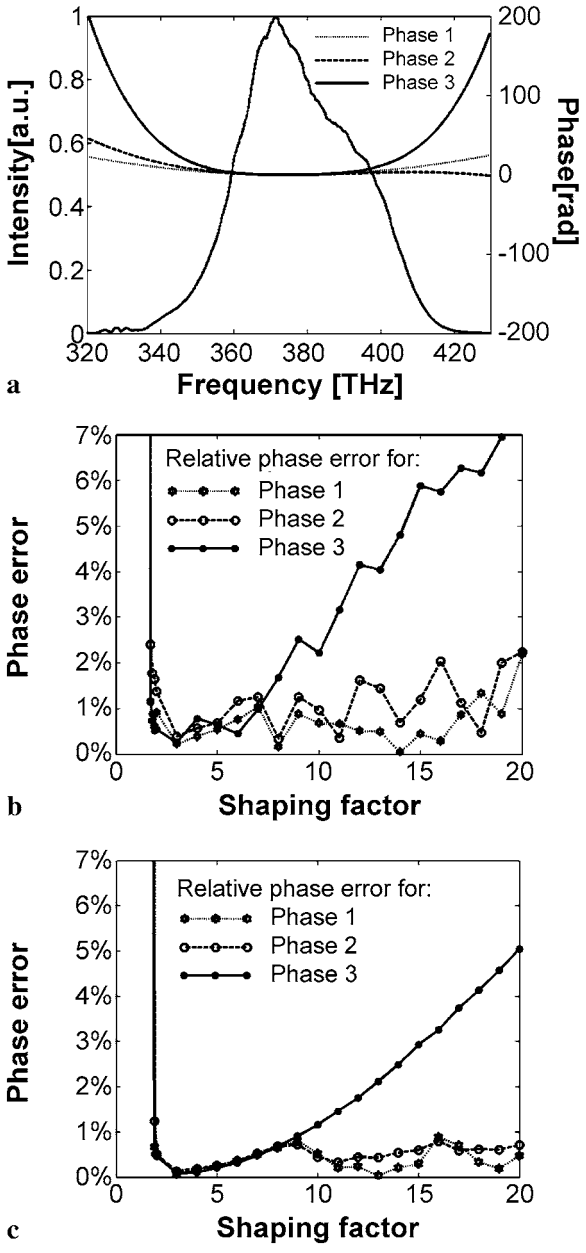

FIGURE 5 Phase errors retrieved from actual spectrum. **(a)** Actual spectrum and assumed phases. **(b)** Retrieved phase errors with different shaping factor for time delay $\tau = 0.7$ ps. **(c)** Retrieved phase errors with different shaping factor for time delay $\tau = 1.0$ ps

a home-made Ti:Sapphire laser, which is not a typical Gaussian. The spectrum is centered at 800 nm with a bandwidth (FWHM) of 81.1 nm (38.5 THz). Figure 5 shows the retrieval errors with different Gabor wavelet shaping factors for this actual spectrum. The spectrum and the assumed spectral phases are shown in Fig. 5a. Figure 5b and c are the retrieved phase errors for different shaping factor for time delay of 0.7 ps and 1.0 ps, respectively.

5 Discussions

The above results show that the high order phase is sensitive to the shaping factors. Apparently the accuracy of the phase retrieval with wavelet-transform analysis is determined by both Heisenberg box and the actual phase. That is, for the rapidly changed spectral phase with frequency, high frequency resolution (small shaping factor) is required.

In the case of phase 1, with a quadratic phase, the ridgeline of wavelet-transform is flat, i.e., the time (period) components have no variations along frequency direction. The spectral shearing interferogram is not a typical "frequency-dependent" signal; therefore, shape of Heisenberg box has no apparent effect on the phase analysis.

In Phase 2, a quadratic plus a cubic phase, the ridgeline of wavelet-transform is tilted; a smaller shaping factor results in a better accuracy. However, for the Phase 3, a more complicated phase, the ridge curve varies remarkably along the frequency direction, and a much higher frequency resolution (smaller shaping factor) is demanded.

Figures 4 and 5b,c show smaller shaping factor tends to fit better range of the spectral phase, which is because frequency resolution degrades as shaping factor increases. On the other hand, the retrieved phase error rises sharply for the shaping factor less than 2, and the phase cannot be extracted at all when the shaping factor is less than 1.5. It is because as the shaping factor is reduced, the time resolution becomes worse.

In general, the shaping factor in the range of $2 \sim 7$ should be reasonable for various signal analysis. For the most widely used Morlet wavelet, the shaping factor is 5; and for the most widely used Gabor wavelet, the shaping factor is $(2 \ln 2)^{-1/2} \cdot 2\pi = 5.336$, which was used in our previous studies [3, 4].

Figures 4 and 5b,c also shows that the value of delay τ does not seem to have big impact on the Phase 1 and Phase 2, but certainly reduces the error for the Phase 3. This is because as the carrier frequency increases, the spectral phase difference loaded on each carrier fringe is decreased; consequently the spacing of the fringe varies tend to be alleviated. It is why a larger carrier frequency (larger delay τ) can reduce retrieved phase error.

It is unfortunate that the shaping factor affects the retrieved phase so much for the rapidly changed and complicated phase, which plays the similar role to the temporal filter in the SPIDER process [5]; however, the uncertainty is essentially different from that resulting from the choice of filter. If we always choose a small shaping factor, for example, $3 \sim 5$ as we suggested, the resulting error is always small enough for various applications. These wavelets have $3 \sim 5$ cycles, the cycles for absolute majority of the popular wavelets (Mexican hat, Morlet, Daubechies, Meyer, Symlets, Coiflets, et al.) all in those range. This has been proved to be reliable, at least for the phase extraction of moderate phase conditions [3, 4].

6 Conclusions

We analyzed the shaping factor of the Gabor wavelet on the accuracy of the phase retrieval for quadratic, cubic, and quartic spectral phases, for the shaping factor from 1 to 20 with both an ideal Gaussian spectrum and a non-typical Gaussian actual spectrum. The results demonstrated that a small shaping factor wavelet (shaping factor range of $2 \sim 7$, more precisely, $3 \sim 5$) is always safe for the phase retrieval of the femtosecond pulses at reasonable conditions listed in the paper. This study may be useful for the on-line feedback phase control of femtosecond optical pulses.

ACKNOWLEDGEMENTS This research was supported in part by China Natural Science Foundation (grant numbers 60178007 and 60490280). The authors thank M. Yamashita, R. Morita, K. Yamane and K. Narita for helpful discussions, and thank the anonymous reviewers for their constructive suggestions.

REFERENCES

1 C.K. Chui (ed.), *An introduction to wavelets* (Academic Press, Boston 1992)
2 S.G. Mallat, *A wavelet tour of signal processing* (Academic Press, New York 1998)
3 Y. Deng, Z. Wu, L. Chai, C. Wang, K. Yamane, R. Morita, M. Yamashita, Z. Zhang, Opt. Express **13**, 2120 (2005)
4 Y. Deng, Z. Wu, L. Chai, C. Wang, Z. Zhang, *Conf. Lasers and Electro-Optics* (Optical Society of America, Baltimore, Maryland 2005) JWB11
5 C. Iaconis, I.A. Walmsley, IEEE J. Quantum Electron. **35**, 501 (1999)
6 M. Takeda, H. Ina, S. Kobayashi, J. Opt. Soc. Am. **72**, 156 (1982)
7 D.J. Kane, R. Trebino, Opt. Lett. **18**, 823 (1993)
8 J.-C. Hong, Y.Y. Kim, Exp. Mech. **44**, 387 (2004)
9 N. Delprat, B. Escudié, P. Guillemain, R. Kronland-Martinet, P. Tchamitchian, B. Torréksani, IEEE T. Inform. Theory **38**, 644, (1992)